Trace element compositions bearing on the origin of large igneous inclusions in ordinary chondrites

A. Ruzicka[1], K.L. Schepker[1], Y. Guan[2]. [1]Cascadia Meteorite Laboratory, Department of Geology, Portland State University, 17 Cramer Hall, 1721 SW Broadway, Portland OR 97207, USA. [2]Division of Geological and Planetary Sciences, California Institute of Technology, Pasadena, CA USA.

INTRODUCTION

Large (multi-mm to cm) igneous-textured inclusions poor in metal and sulfide occur in ~4% of ordinary chondrites [1] and hold important clues for early heating processes in the solar system. Most have major-element compositions and oxygen isotopic compositions broadly similar to chondrules, and fall into two main chemical types, relatively unfractionated (*Unfr*) and vapor fractionated (*Vfr*). These appear to have formed by melting of chondritic material with (*Vfr*) or without (*Unfr*) chemical exchange with nebular gas [2,3]. Other inclusions have distinctly different compositions and could have been produced dominantly by igneous differentiation [4]. We used the Cameca 7f-Geo ion microprobe at Caltech using an energy filtering technique [5] to determine the concentrations of 37 elements in 2 *Unfr* and 7 *Vfr* inclusions in various type 3-6 ordinary chondrites (Table 1), obtaining the largest trace element data set yet obtained for such materials. The compositions of all principal phases were measured, and modal reconstruction was used to determine bulk compositions.

Context

- **Among *Unfr* inclusions analyzed with SIMS, both 7871-I1 and 8645-I1 are texturally integrated with their hosts implying *in situ* metamorphism. Both have L-like chondrite-like Fe/Mg silicate compositions, but oxygen isotopic compositions more consistent with the H-group and L-group, respectively, suggesting derivation from different source regions [3].**
- **Among *Vfr* inclusions analyzed with SIMS, all have variable Fe/Mg silicate compositions (in Tdk-I1 only pyroxene is variable, olivine is uniform), suggesting they were not significantly metamorphosed *in situ*. As typical for *Vfr* inclusions in type 3 hosts, MET-I1 and MET-I3 have O-isotope compositions that lie well outside of ordinary chondrite fields with $\Delta^{17}O$ values falling between H chondrites and the TF line, suggesting exchange with nebular gas of distinctive composition [3].**

Bulk Compositions

Fig. 2 Bulk compositions projected on pseudoternary liquidus diagram olivine (Ol) – quartz (Qz) – plagioclase (Pl).

• All inclusions in the larger study shown; inclusions studied by SIMS are designated.

• Bulk compositions cluster around ordinary chondrite (OC); all inclusions have olivine on liquidus.

• No evidence these inclusions originated by igneous differentiation; instead, their compositions suggest derivation from chondritic material, with mostly modest chemical fractionation.

Fig. 2

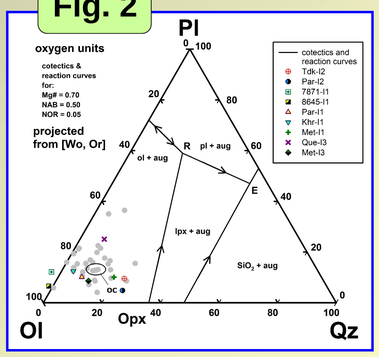

Fig. 3

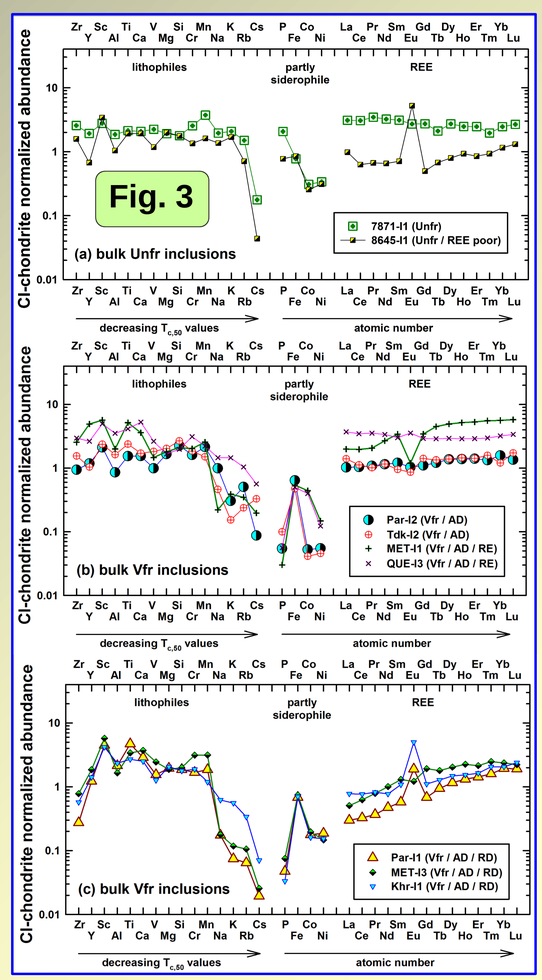

< Fig. 3 Cl-chondrite-normalized bulk compositions of inclusions studied with SIMS. Errors bars have been omitted for clarity.

• Trace element data confirm previous *Unfr* and *Vfr* chemical groupings, but provide evidence for subgroups.

• *Unfr* inclusion 7871-I1 (Fig. 3a) has nearly unfractionated abundances of all lithophile elements and P, being depleted only in the partly siderophile elements Fe, Co, Ni and highly volatile Cs.

• *Unfr* inclusion 8645-I1 (Fig. 3a) has relatively unfractionated abundances for most elements, but is depleted in REE (except for Eu), Y, and P. These depletions suggest removal of a phosphate component, which can generate "W-shaped" REE patterns [6].

• Tdk-I2 and Par-I2 (Fig. 3b) have noticeable alkali depletions (designated *Vfr / AD,* vapor-fractionated/alkali-depleted); REE are at chondritic levels. Their compositions can be explained by loss of the volatile alkali elements.

• MET-I1 and QUE-I3 are depleted in alkalis and enriched in refractory elements (Zr-Ca and REE) (Fig. 3b) (designated *Vfr / AD / RE,* alkali-depleted, refractory-enriched). REE abundances are relatively flat but enriched for QUE-I3, and HREE-enriched with negative Eu anomaly for MET-I1 (Fig. 3b). These compositions suggest high-temperature condensation/evaporation, with the REE pattern for MET-I1 attributable to loss of a feldspar component relative to mafic minerals, consistent with a negative Al anomaly (Fig. 3b).

• The remaining 3 inclusions, Par-I1, MET-I3, and Khr-I1 have distinctive bulk compositions. A common feature is a strong depletion of alkali elements and the most refractory elements (Zr, Y), with abundance maxima for elements of more intermediate volatility (Sc-Mn) (Fig. 3c). These inclusions are thus both alkali depleted and refractory depleted (*Vfr / AD / RD*), a signature that can be explained by fractional condensation, involving removal of both a refractory and volatile component. The inclusions have HREE-enriched patterns attributable to loss of a feldspar component relative to mafic minerals (consistent with negative Al anomaly). However, Par-I1 and Khr-I1 also have positive Eu anomalies that cannot be explained by loss of feldspar. Instead, it is suggested that Eu is enriched relative to other REE as a result of fractional condensation. If correct this would imply condensation occurring at a temperature below which most REE, except for the relatively volatile Eu, had condensed.

Table 1

List of inclusions studied by SIMS

Inclusion	Chemical type	Host
7871-I1	*Unfr*	NWA 7871 (L6)
8645-I1	*Unfr / REE poor*	NWA 8645 (L6)
Khr-I1	*Vfr / AD / RD*	Khohar (L3.6)
MET-I1	*Vfr / AD / RE*	MET 00489 (L3.6)
MET-I3	*Vfr / AD / RD*	MET 96515 (L3.6)
Par-I1	*Vfr / AD / RD*	Parnallee (LL3.6)
Par-I2	*Vfr / AD*	Parnallee (LL3.6)
QUE-I3	*Vfr / AD / RE*	QUE 97008 (L3.05)
Tdk-I2	*Vfr / AD*	Tamdakht (H5)

Textures

Fig. 1 False color BSE-EDS SEM images showing five inclusions analyzed with SIMS.

• Par-I2 is a pyroxene-rich drop-formed object whereas nearby Par-I1 is a fragment of a larger mass (Fig. 1a). Both are microporphyries. Note smaller regular chondrules between.

• Tdk-I2 is a pyroxene-rich fragment with some olivine bars (Fig. 1b). Note smaller, regular-sized chondrules at upper right.

• 8645-I1 (Fig. 1c) and 7871-I1 (Fig. 1d) are olivine-rich microporphyries; much more phosphate (orange) occurs in 7871-I1 than in 8645-I1.

Fig. 1

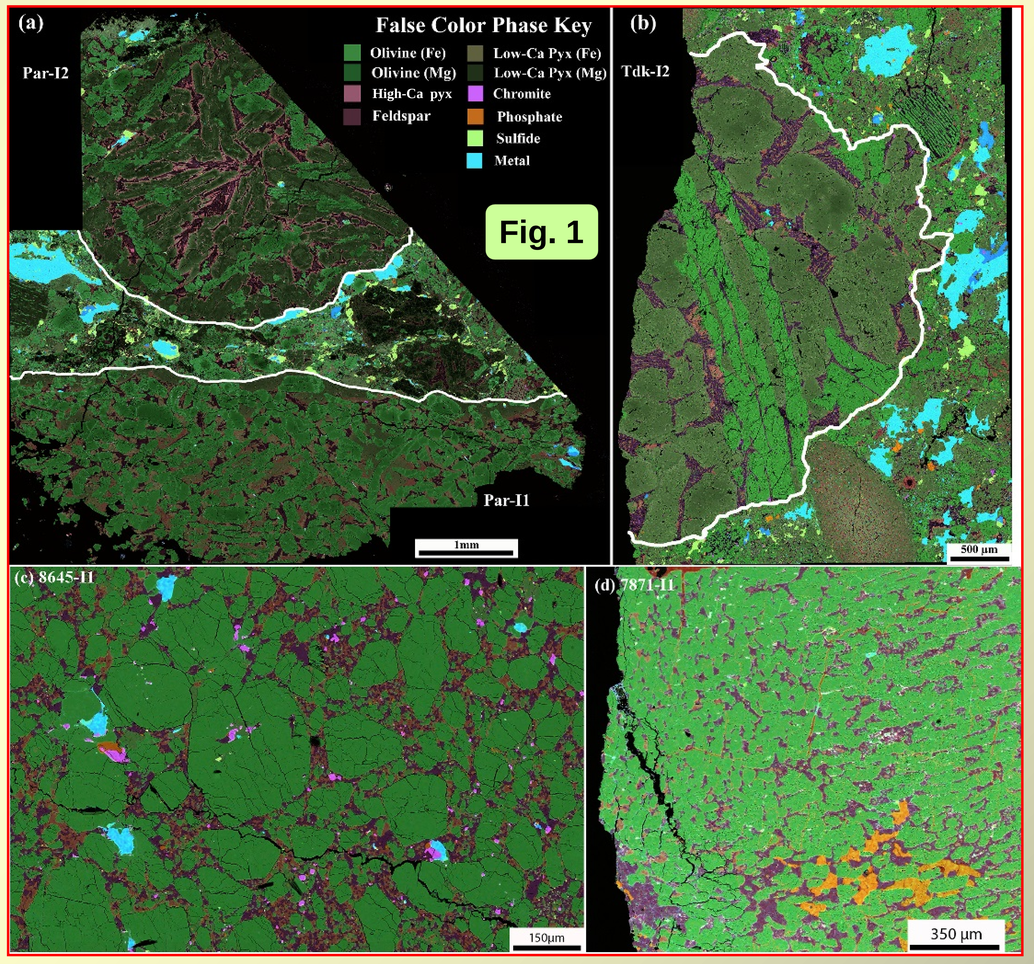

Phase Compositions

Fig. 4

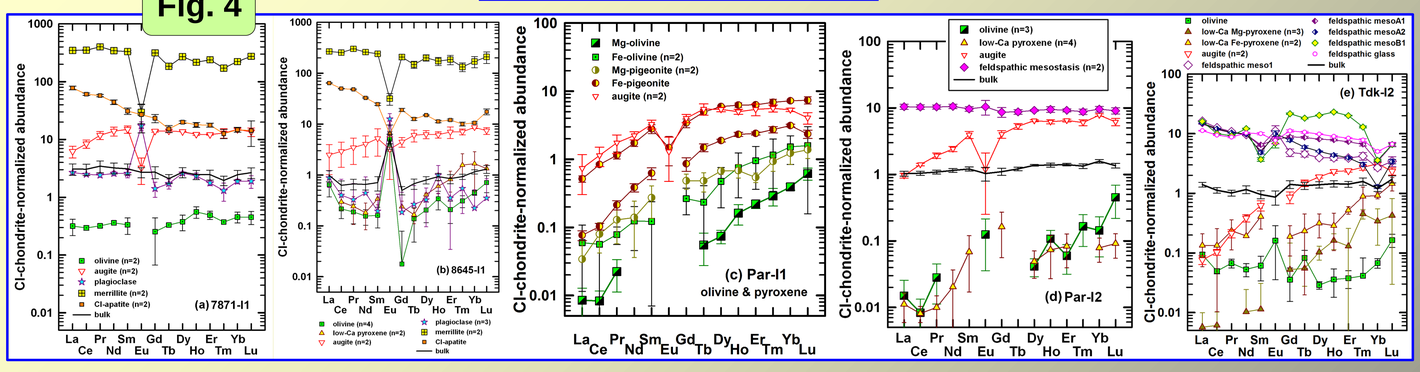

^ Fig. 4 Cl-chondrite-normalized REE abundances in phases from five inclusions studied with SIMS. Error bars represent counting errors or standard deviations, whichever is larger.

• 7871-I1 and 8645-I1 show evidence for metamorphic equilibration but in different ways. In 7871-I1, olivine has nearly uniform REE abundances (Fig. 4a) likely caused by metamorphic equilibration, and other phases have compositions not unexpected for either igneous or metamorphic processes. 8645-I1 is very different, with olivine, plagioclase, and low-Ca pyroxene all having similar compositions that resemble the bulk "W-shaped" pattern, including huge positive Eu anomalies (Fig. 4b). No inclusions in these phases that could for these patterns are observed. Instead, all were evidently equilibrated to roughly the same composition, likely as a result of sequestration of REE in phosphate (in particular, merrillite).

• In Par-I1, igneous fractionation effects are prominent in olivine and pyroxene (Fig. 4c) and plagioclase (not shown). Measured REE abundances resemble igneous patterns and increase systematically in the sequence Mg-olivine, Fe-olivine, Mg-pigeonite, Fe-pigeonite and augite, suggesting this inclusion experienced closed system crystallization from a nearly complete melt.

• Par-I2 olivine and pyroxene have similar and low REE abundances (Fig. 4d) with no obvious differences between magnesian and ferroan grains that are locally reversely zoned, suggesting disequilibrium. Augite contains a small but distinct positive Eu anomaly. The positive Eu anomaly in augite suggests exchange with a vapor enriched in this relatively volatile REE, implying high temperatures, but the relatively unfractionated bulk composition of the inclusion is inconsistent with a high temperature origin for the inclusion overall. These data can be explained by partial melting in a brief but intense heating that allowed exchange between gas and melt during augite crystallization, but which did not allow equilibrium to be maintained in the less-melted ultramafic residua.

• In Tdk-I2, interstitial feldspathic phases show a variety of patterns, including glass with negative Eu and Yb anomalies (Group III pattern), and some portions of mesostases with super-refractory patterns characterized by mostly high HREE and low Eu, Yb and Sm (Fig. 4e). These data unambiguously indicate high-temperature processing and exchange with vapor during intense evaporative melting. However, bulk REE contents are close to chondritic (~0.9-1.7 x CI) (Fig. 4e), which indicates that Tdk-I2 is not very refractory overall. Olivine has an irregular, non-igneous pattern. Although pyroxene shows evidence for fractional crystallization, there is also an offset pattern between LREE and HREE for ferroan grains (Fig. 4e). These data can be reconciled by a brief but intense evaporative melting event that partly melted the inclusion and created a refractory mesostasis, and which chemically disturbed the ultramafic residua.

CONCLUSIONS

1) **The two *Unfr* inclusions 7871-I1 and 8645-I1 could have formed by melting of chondritic materials and metamorphic equilibration.**
2) **The *Vfr* inclusions Par-I2 and Tdk-I2 probably formed by evaporative melting during brief events that chemically disturbed the ultramafic residua but which did not result in highly refractory objects overall.**
3) **Three other *Vfr* inclusions including Par-I1, MET-I3, and Khr-I1 likely formed as fractional melt condensates.**
4) **The data support the idea that *Vfr* inclusions formed in a space environment.**

References: [1] Bridges J.C. and Hutchison R. (1997) *MAPS* 32, 389-393. [2] Armstrong K. (2014) MS Thesis, Portland State University. [3] Ruzicka A. et al. (2016) 47th LPSC, Abstract #2230. [4] Ruzicka A. et al. (2012) *MAPS* 47, 1809-1829. [5] Zinner E. and Crozaz G. (1986) *Int. J. Mass Spectr. Proc.* 69, 17-38. [6] Ruzicka et al. (2005) *MAPS* 40, 261-295.

Acknowledgments: NASA grant support for this work (Grant NNH12ZDA001N), and helpful discussions with Christine Floss, are gratefully acknowledged.

Abstract 2477, 48th Lunar and Planetary Science Conference (2017).